ELSEVIER

Catalysis Today 77 (2003) 335–346

CATALYSIS TODAY

www.elsevier.com/locate/cattod

# Combustion of $CH_4$ over a $PdO/ZrO_2$ catalyst: an example of kinetic study under severe conditions

G. Groppi*

*Dipartimento di Chimica, Materiali e Ingegneria Chimica, CMIC, Politecnico di Milano, Piazza Leonardo da Vinci 32, Milan 20133, Italy*

## Abstract

A kinetic study on $CH_4$ combustion over a very active $PdO/ZrO_2$ catalyst with high Pd loading (10% w/w of Pd) is presented as an example of a demanding problem which requires both the development of appropriate experimental tools and a theoretical insight on surface chemistry.

The use of an annular catalytic reactor as a tool to collect kinetic data under unusually severe conditions (high temperature and $CH_4$ concentration) is described in comparison with the use of a conventional packed bed reactor. In particular, problems related to the biasing effects of mass, heat and momentum transfer are addressed.

Kinetic data addressing the effects of $CH_4$, $O_2$, $H_2O$ and $CO_2$ concentration in a temperature range from 400 to 550 °C are analysed by means of a purely empirical power law model and of a formal kinetic model based on literature indication assuming methane dissociative adsorption as the rate controlling step.

*Keywords:* Catalytic combustion; $PdO/ZrO_2$ catalyst; Kinetics; $CH_4$ combustion; Annular reactor

## 1. Introduction

The classical statement of “catalysis as a kinetic phenomenon” [1] well emphasises the pivotal importance of collection and analysis of kinetic data in catalyst science and technology. Correlation of reaction rate data may be sought for both engineering and fundamental purposes. Engineers need rate equations to be implemented in mathematical model of catalytic reactors which can be used both for design purposes and to predict the effect of reactor operating changes on performances. Fundamental scientists need a rational assessment of reaction rate data: for systematic evaluation of the effect of variation of catalyst composition; to gain insight, although indirect, on the reaction mechanism and eventually to provide assistance in the development of novel catalyst formulations.

Despite, the above statements have been quite universally recognised since a long time, the field of catalytic kinetics is still quite stimulating from a fundamental point of view and far from being exhaustively understood. On the other hand, the applied research of more active and selective catalysts would stringently requires more physically sound kinetic description of catalytic reactions [2].

In this paper a kinetic study on an apparently simple reaction, the complete oxidation of $CH_4$ to $H_2O$ and $CO_2$ over a PdO-supported catalyst, is presented as an example of the still critical need of both novel experimental tools, able to provide kinetic data under the severe conditions which are often relevant to practical applications, and deeper theoretical understanding of the complex chemistry undergoing onto the catalyst surface.

---

* Tel.: +39-2-23993258; fax: +39-2-70638173.
*E-mail address:* gianpiero.groppi@polimi.it (G. Groppi).

PII: S0920-5861(02)00378-4

In view of its high activity supported PdO is the catalyst of choice for $CH_4$ combustion in applications which require low light-off temperatures such as exhaust treatment from compressed natural gas engines [3] and catalytic combustors for gas turbines with ultra-low emissions of $NO_x$, CO and unburned $CH_4$ [4]. Particularly in this latter case, $ZrO_2$-supported catalysts with high palladium loading (about 10% w/w of Pd) were reported to posses the required activity and stability properties to be used in commercial combustors [5]. Although several studies are reported in the literature on $CH_4$ combustion kinetics over Pd catalysts [6–12] very few data are available for temperatures higher than 400 °C [13], which, however, are of practical interest [4].

In the following the preparation of a powder catalyst to be used in a conventional packed bed reactor and the results of $CH_4$ combustion activity tests are first presented. Then the characteristics and the preparation method of an annular flow reactor able to overcome experimental limitations of packed beds are illustrated. Finally, the results of kinetic measurements performed with the annular reactor over a wide range of experimental variables and their analysis using a power law and a formal model based on mechanism assumptions are presented and discussed.

## 2. Experimental

### 2.1. Packed bed

#### 2.1.1. Preparation and characterisation of powder catalysts for packed bed tests

For activity tests in a conventional packed reactor a $PdO/ZrO_2$ (10% w/w of Pd) catalyst was prepared in powder form according to the following procedure. The $ZrO_2$ support powders were obtained by calcining $Zr(OH)_4$ (Mel Chemicals, mean particle size = 1 μm) at 950 °C. Upon calcination the support consisted of a single phase monoclinic $ZrO_2$ (m-$ZrO_2$), as revealed by the XRD analysis, with a BET surface area of 15 $m^2/g$, a pore volume of 0.124 $cm^3/g$ and an average pore radius of 23 nm.

The $ZrO_2$ powders were dry-impregnated with a 10% $Pd(NO_3)_2$ aqueous solution (Alfa-aesar) and then dried at 110 °C for 2 h. The impregnation procedure was repeated several times until Pd metal loading achieved 10% w/w. The catalyst powders were then calcined at 600 °C in air for 10 h in a muffle furnace in order to achieve complete decomposition of $Pd(NO_3)_2$ to PdO. XRD spectrum upon calcination evidenced the presence of crystalline PdO along with the m-$ZrO_2$ support. For the activity tests 100 mg of finely grinded powders (140–200 mesh) were loaded in a quartz microreactor. The catalyst powders were thoroughly mixed with inert quartz powders of the same particle size ($W_{cat}/W_{dil} = 1/2$) to reduce temperature gradients associated with the strong combustion enthalpy. The catalyst temperature was measured by a fixed thermocouple (type K) located in the catalyst bed. The reactor was fed by a 250 $cm^3$/min at STP (GHSV = 150 000 $cm^3/g_{cat}$ h at STP) flow mixture consisting of 0.5% $CH_4$, 4% $O_2$, He to balance.

Activity tests were performed by temperature programmed (TP) experiments (heating/cooling rate = 15 °C/min). Analysis of products and reactants were performed by on-line mass spectroscopy (Baltzers QS422), which allowed for continuous determination of $CH_4$ conversion.

### 2.2. Annular reactor

#### 2.2.1. Concept and design

To collect kinetic data under severe conditions an annular flow reactor was adopted [13–15]. Such a catalytic reactor, which is sketched in Fig. 1, consists

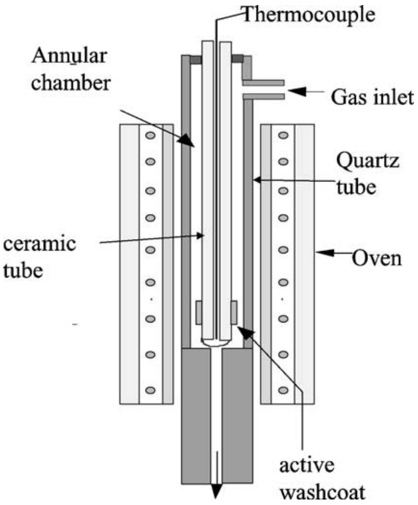

Fig. 1. Schematic diagram of the annular catalytic reactor.

of a ceramic tube co-axially placed within a quartz tube. The reacting gases flow in the annulus between the two tubes contacting a thin catalyst layer which is deposited onto the external surface of the dense ceramic tube. Thanks to the straightforward pattern of the flow, a laminar regime can be preserved up to high specific flow rate thus maintaining limited pressure drops. Combining this with the possibility to minimise the catalyst loading by controlling the thickness and the length of the catalyst layer, extremely short contact times can be achieved with negligible pressure drops.

In view of the well-defined geometry and flow pattern, mathematical modelling was effectively used to design the reactor geometry so as to guarantee a minimum impact of diffusional limitations on kinetic data. Details on the mathematical model and on the simulation results are reported elsewhere [13,16], however, as shown in Fig. 2, the theoretical design pointed out the thickness of the catalyst layer as the most critical parameter. At the very high reaction rate achieved by $CH_4$ combustion in the mid-high temperature range (500–600 °C) over heavily Pd loaded catalysts, active coating layers as thin as 15 μm are required to keep the overall efficiency of the reactor above 80%, i.e. to keep the error on the estimate of the kinetic constant when neglecting the impact of diffusional limitations below 20%. Also the size of the annular gap must be kept in the order of few hundreds of micron to avoid the onset of serious limitations associated with both gas–solid diffusion and axial diffusion in the gas phase.

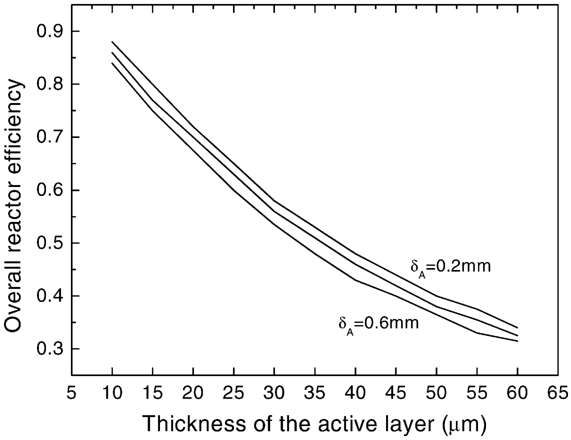

Fig. 2. Calculated overall efficiencies of the annular flow reactor due to mass transfer limitations.

### 2.2.2. Deposition and characterisation of the catalyst layer

The need to obtain an adherent catalyst layer with a uniformly thin thickness, good adhesion and appropriate morphological and catalytic properties requires the development of a specific preparation/deposition technique of the catalyst layer. For the specific application herein investigated and, in general, for the investigation of very fast reactions, this is not a drawback since industrial applications are typically operated on structured catalysts obtained by deposition of an active layer onto pre-shaped geometrical/mechanical supports (honeycombs, plates, foams, etc.) [4]. Accordingly, the same catalyst coating deposition technique adopted for the preparation of commercial structured catalysts can be used for the annular reactor.

In this work the wash-coating procedure adopted for the deposition of the catalyst layer was derived starting from patent literature indications [17] by a careful tuning of the following preparation parameters: (i) selection of the precursor catalyst powders; (ii) composition and mixing of the slurry to be deposited; (iii) withdrawal velocity of the ceramic tube during dipping deposition; (iv) drying and calcination upon deposition.

The precursor catalyst powder was obtained by calcination of $Zr(OH)_4$ at 500 °C for 10 h, followed by repeated dry impregnation with $Pd(NO_3)_2$ up to 10% w/w of Pd with a final calcination at 500 °C. The calcined powder was suspended in a $HNO_3$ aqueous solution to obtain a slurry with the following composition: $H_2O$/powder $=$ 2.1 g/g, $HNO_3$/powder $=$ 1.7 mmol/g. The slurry was then ball-milled for 24 h using zirconia spheres ($d = 1$ cm). The ceramic $\alpha$-$Al_2O_3$ tube (outer radius, $r_i = 3.25$ mm) was wash-coated by dipping into the slurry with a constant withdrawal velocity of 3 cm/min. After flash heating at 280 °C for 5 min, the tube was calcined at 800 °C for 10 h under air flow of 10 $cm^3$/min (at STP). Length, weight and density of the catalyst layer deposited on $\alpha$-$Al_2O_3$ tube were 10 mm, 6 mg and 2 $g/cm^3$, respectively. The catalyst thickness estimated by optical microscopy was 15 μm.

Morphological properties of the catalyst were analysed by $N_2$ adsorption/desorption at 77 K (CarloErba Sorptomatic 1900 series) and Hg-porosimetry. PdO/$ZrO_2$ exhibited a bimodal pore distribution consisting of mesopore ($\varepsilon_P = 0.1$, $\bar{r}_p = 28\,\mathrm{nm}$) and macropores ($\varepsilon_P = 0.13$, $\bar{r}_p = 64\,\mathrm{nm}$).

The catalytically coated α-$Al_2O_3$ tube was placed within a quartz tube with an inner radius of 3.5 mm so as to obtain an annular chamber with an average height of 250 μm. The axial temperature profile was measured using a K-type thermocouple sliding within the internal cavity ($d = 2\,\mathrm{mm}$) of the α-$Al_2O_3$ tube. Such a thermocouple provides a measurement of the catalyst temperature under the reasonable assumption of thermal equilibrium on the cross-section of the ceramic tube.

Analyses of reactants and products were performed by an on-line GC (Hewlett Packard, HP6890 Series) equipped with a 5 Å molecular sieve column for separation of $O_2$, $N_2$, $CH_4$ and CO and with a PORAPAK-Q column for separation of $CH_4$, $CO_2$ and $H_2O$. Concentration of the single species was determined with two parallel thermal conductivity detectors (TCDs). Activity tests were performed under steady-state conditions collecting one average conversion point by four repeated GC analyses during a 90 min hold at each temperature.

## 3. Results and discussion

### 3.1. Packed bed reactor

In Fig. 3 conversion data obtained in two repeated TP cycle between 150 and 500 °C are reported. The lack of hysteresis between heating and cooling ramp provides an indication that nearly steady-state conditions were achieved under the investigated conditions. Besides the good reproducibility exhibited by the repeated thermal cycles indicates that the catalyst was stable within the investigated temperature range. Conversion curves show that the reaction starts just above 200 °C, reaching 10% conversion at about 250 °C. Then the conversion rapidly increases achieving practically 100% (>99%) just below 400 °C. Above this temperature no further indications on combustion kinetics could be collected since conversion was fixed at 100%; accordingly only a lower limit to the actual reaction rate can be obtained. This is a serious limitation since in industrial applications much higher temperature range are of practical interest, e.g. 450–850 °C for gas turbine catalytic combustors.

In principle one can operate the packed bed reactor at significantly shorter contact times in order to shift the 100% conversion limit at higher temperatures so as to enlarge the investigation range. However,

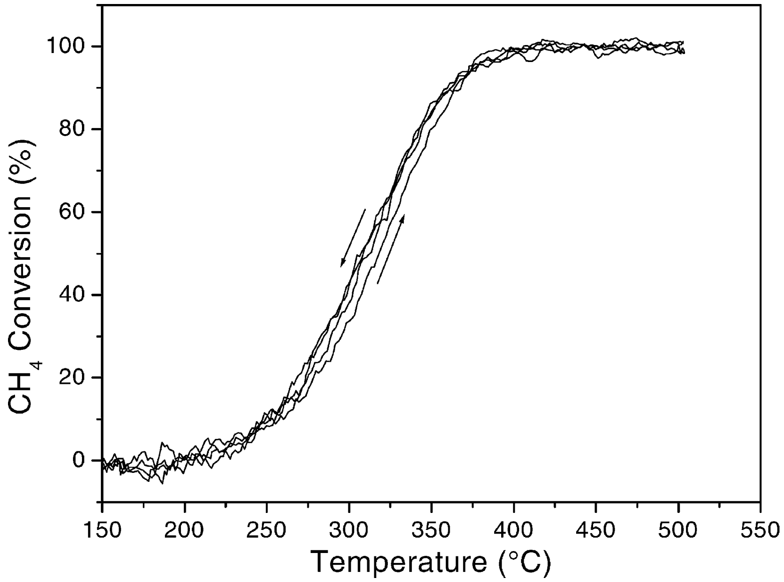

Fig. 3. TP combustion curves of $CH_4$ over PdO/$ZrO_2$ in a packed bed reactor at GHSV $= 1.5 \times 10^5\,\mathrm{cm^3/g\,h}$ at STP.

several reasons would discourage such an attempt. First pressure drop would rapidly became a critical issue: indeed under the investigated conditions pressure drops up to 0.5 bar were observed which would linearly increase with the flow rate. Such a problem is strictly related to the necessity to keep the particle size of the catalyst powders as small as possible in order to minimise the impact of diffusion limitations. In the investigated conditions, despite of the small average particle size (95 μm) of the catalyst powder, classical diagnostic criteria [18] for the onset of intraparticle diffusion were tightly satisfied: at 375 °C a value of the dimensionless group $R_{obs}r_p^2/D_{eff}C_S$ of 0.3 was calculated. Considering an apparent activation energy of 82.4 kJ/mol, that has been derived from the conversion data using a first-order kinetics and is in line with literature values obtained under the same assumption, the theoretical safety limit ($R_{obs}r_p^2/D_{eff}C_S \leq 1$) would be rapidly overcome as soon as the temperature exceeds 400 °C. On the other hand, a further decrease of the smaller particle size would make pressure drops even more critical. Besides, it is difficult to handle and confine very fine powders within the reactor.

Another critical issue is associated with the temperature distribution within the reactor. The criterion for negligible temperature gradients in the catalyst bed [18] was already largely overcame under the investigated conditions: at 375 °C a value of the dimensionless group $\frac{E_{act}}{R_g T^2} \cdot \frac{R_{bed} r_t^2 \cdot (-\Delta H_R)}{k_{eff}}$ in excess of 3 was calculated. Also in this case the usual remedy of increasing the dilution ratio could be applied to a limited extent since it would result in an increase of the bed height and, consequently, of the pressure drop.

## 3.2. Annular reactor

### 3.2.1. Reactor performances

To overcome the limitations discussed above, $CH_4$ combustion tests have been performed in an annular flow catalytic reactor. Fig. 4 reports the conversion curve obtained in the temperature range 400–550 °C under the following standard conditions: feed = 0.8% $CH_4$, 21% $O_2$, $N_2$ to balance, pressure = 1 atm, flow rate = 100 cm$^3$/min at STP. Thanks to the extremely high GHSV ($10^6$ cm$^3$/g$_{cat}$ h at STP), $CH_4$ conversions lower than 60% were obtained in the investigated temperature range, i.e. far below the 100% limit achieved already at 400 °C in the packed bed tests. It is worth noting that with the annular reactor the upper

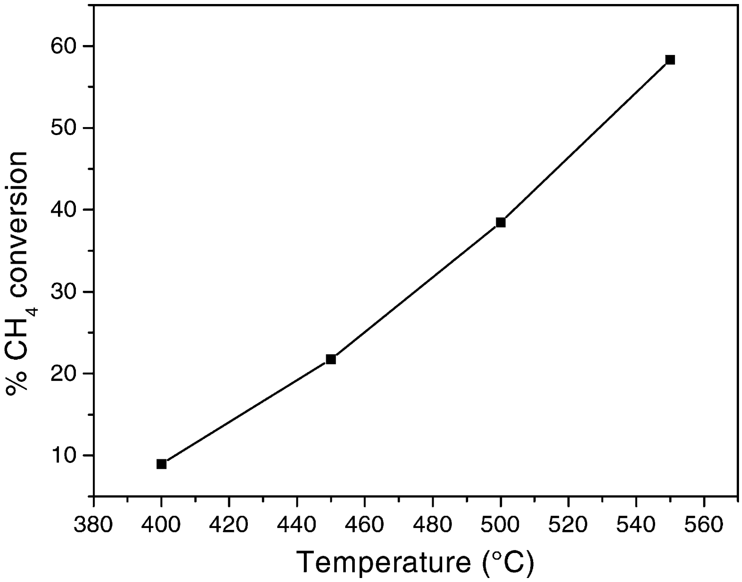

Fig. 4. Steady-state conversion curve in the annular flow reactor at standard conditions GHSV = $10^6$ cm$^3$/g h at STP, feed = 0.8% $CH_4$, 21% $O_2$, $N_2$ carrier, pressure = 1 atm.

limit to the investigated temperature was set by previous experiments on catalyst stability showing the presence of significant catalyst deactivation at 600 °C in the presence of feed $H_2O$. Conversion values in Fig. 4 shows that the reactor has potential to provide kinetic data at higher temperatures corresponding to faster reaction rate, particularly when considering that the flow rate and, consequently, the GHSV can be further enhanced since actual pressure drops under the investigated conditions were below 0.1 bar. Besides experiments performed using He as the inert gas provided the same conversion values obtained in standard tests (inert gas $N_2$) confirming that, in line with the prediction of the mathematical model design of the reactor, the impact of diffusion limitations was negligible under the investigated conditions thanks to the very small thickness of the catalyst layer.

The measured axial thermal profiles showed that temperature differences along the catalyst bed were kept below 5 °C even at 60% conversion, which can be assumed as isothermal conditions with respect to other experimental uncertainties. During tests performed under more severe conditions, up to 3% of $CH_4$ in the feed, measured temperature gradients were always maintained within reasonable limits (typically $\Delta T < 10\,°C$) confirming the high dissipation efficiency of reaction heat allowed by the annular reactor that, as showed by more detailed investigations [15,16], is mainly due to radiation from the catalyst skin.

### 3.2.2. Kinetic study

In conclusion, the above results confirmed the potential of the annular reactor to collect kinetic data under much more severe conditions than those allowed by conventional packed bed reactors. In view of this an extensive kinetic study was performed including the effect of concentration of reactants and products covering the following ranges of experimental variables: $T = 400$–$550\,°C$, GHSV $= 10^6\,cm^3/g_{cat}\,h$ at STP, feed composition: $O_2 = 11.5$–$21.2\%$, $CH_4 = 0.4$–$3.2\%$, $H_2O = 0$–$3.5\%$, $CO_2 = 0$–$2.7\%$ and $N_2$ to balance.

Under the investigated very lean conditions (equivalence ratio below 0.3) no effect of $O_2$ concentration was observed in line with previous literature report [8,10,11,13]. On the other hand, significant effects of $H_2O$, $CO_2$ and $CH_4$ were found and are plotted in Figs. 5–7, respectively (dots). $H_2O$ was found to hinder $CH_4$ combustion over all the investigated temperature range. Such inhibition effect was previously reported by several authors in the literature [9–13,19,20], but its extent in the high temperature

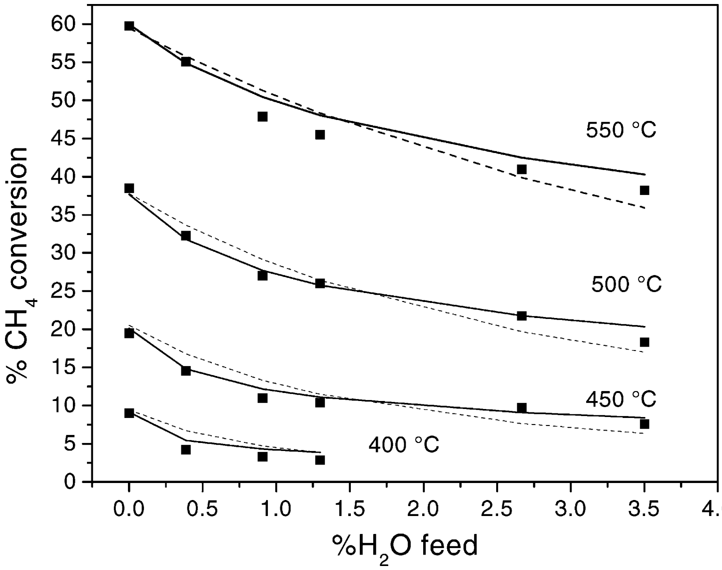

Fig. 5. Effect of $H_2O$ concentration. Standard operating conditions except of $H_2O$ concentration. Dots: experimental points; solid lines: data fitting with power law model (5); dashed lines: data fitting with the formal model (6).

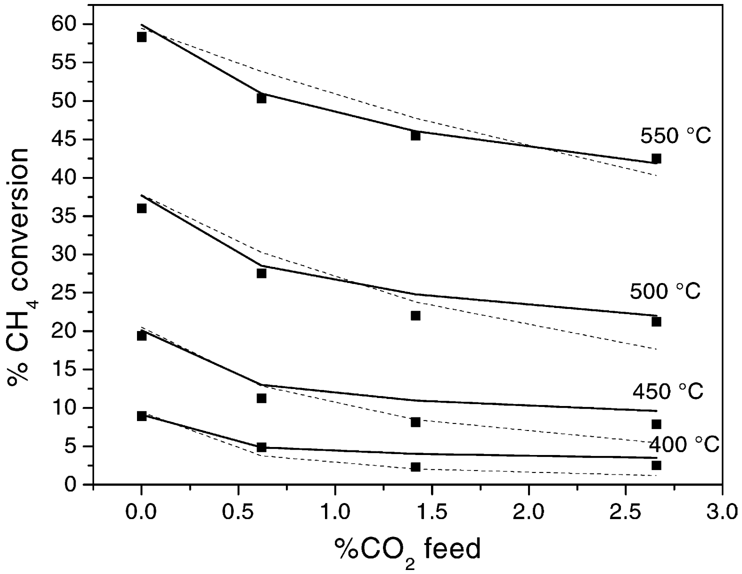

Fig. 6. Effect of $CO_2$ concentration. Standard operating conditions except of $CO_2$ concentration. Dots: experimental points; solid lines: data fitting with power law model (5); dashed lines: data fitting with the formal model (6).

range of practical interest was argued [21]. The results herein presented, confirmed that water still inhibits combustion up to 550 °C, in line with recent reports from the same lab [13], concerning data collected with a similar annular reactor over a γ-$Al_2O_3$-supported PdO catalyst, and with qualitative evidences reported by Ciuparu and Pfefferle [22] for a $ZrO_2$-supported catalyst.

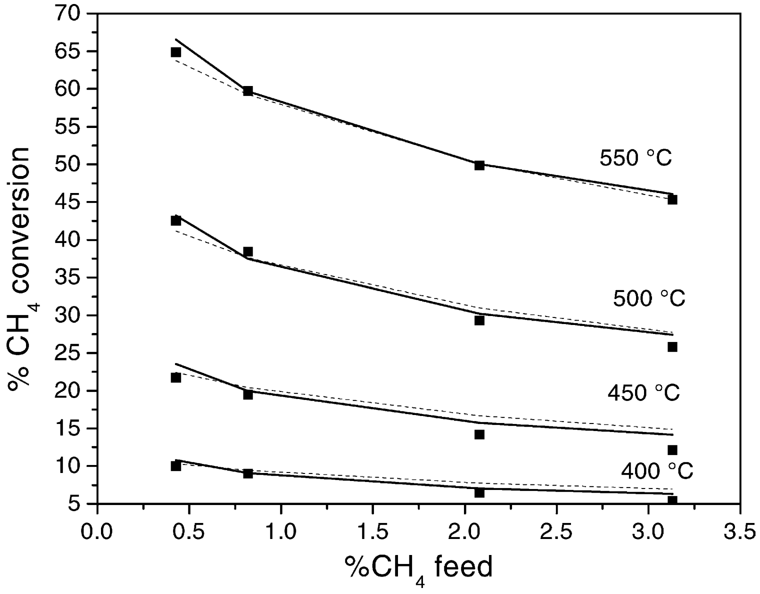

Fig. 7. Effect of $CH_4$ concentration. Standard operating conditions except of $CH_4$ concentration. Dots: experimental points; solid lines: data fitting with power law model (5); dashed lines: data fitting with the formal model (6).

Literature data on $CO_2$ inhibition are much more controversial since some authors did not find any inhibition effect [7,11], whereas others observed it only at high $CO_2$ concentration [9,10,19]. The results herein reported show a $CO_2$ inhibition effect similar to that of $H_2O$. Such discrepancy with respect to several literature reports cannot be simply associated with the higher temperature range investigated in the present study. Indeed no $CO_2$ effects were observed in a similar temperature range over a $PdO/\gamma\text{-}Al_2O_3$ catalyst [13]. Accordingly, a role of the support has to be likely invoked as partly responsible for the catalyst behaviour against $CO_2$ inhibition.

Finally, Fig. 7 shows that at a given temperature conversion decreases on increasing $CH_4$ inlet concentration. This is not at variance to literature indications, typically reporting a first-order dependence on $CH_4$ concentration of the combustion rate [8–13], since it can be associated with the inhibiting effect of the products whose concentrations at given conversion increase with the inlet molar fraction of $CH_4$.

The conversion data discussed above were fitted by testing different kinetic expressions. The following simple 1D, pseudo-homogeneous, isothermal model was adopted for the simulation of the annular reactor:

$$F\frac{\mathrm{d}Y_{CH_4}}{\mathrm{d}W_{cat}} = -r \tag{1}$$

$$Y_{CH_4} = Y^0_{CH_4} \text{ at } z = 0 \tag{2}$$

where $F$ is the molar flow rate (cm$^3$/s at STP), $W_{cat}$ the catalyst weight (g), $Y_{CH_4}$ the $CH_4$ molar fraction and $r$ the combustion rate (cm$^3$/g$_{cat}$/s at STP).

The use of such a simple model is consistent with the results of the reactor design by mathematical modelling showing that the impact of all the relevant mass transfer effects (intraporous internal diffusion; gas–solid external diffusion; axial diffusion in the gas phase) can be neglected without significant errors on the estimates of the kinetic constants.

The ordinary differential equation (1) at the initial condition (2) was solved using an explicit Runge–Kutta method. The ODE solver was incorporated into the robust global nonlinear regression routine BURENL [23,24] to obtain the parameter estimates and statistical analysis of the results. Regression was performed on a set of 53 experimental data.

To minimise correlation among the parameters, the following classical re-parameterisation of the kinetic and thermodynamic constants within the different tested rate expressions was adopted

for kinetic constant :

$$k_j = \exp\left[\beta_{j,1} - \beta_{j,2}\left(\frac{1000}{T} - \frac{1000}{673}\right)\right] \tag{3}$$

for thermodynamic constants :

$$K_i = \exp\left[\beta_{i,1} + \beta_{i,2}\left(\frac{1000}{T} - \frac{1000}{673}\right)\right] \tag{4}$$

The following empirical power law expression was first tried:

$$r\ (\mathrm{cm^3/g_{cat}/s\ at\ STP}) = \frac{k_c P_{CH_4}}{P^a_{H_2O} P^b_{CO_2}} \tag{5}$$

With partial pressure $P_i$ in bar.

In expression (5) oxygen reaction order was fixed to 0 in line with the experimental results collected in this work, whereas reaction order with respect to $CH_4$ was constrained to 1, consistently with previous literature indications. Table 1 provides the estimate of the four parameters (note that the temperature-dependent kinetic constant was rewritten in the re-parameterised form (3)) along with some statistical indexes. Data fitting is also shown in Figs. 5–7 (solid lines) and in the parity plot reported in Fig. 8 (square points). As a general comment the quality of the fitting is satisfactory. Inspection of Figs. 5–8 does not show any systematic deviation from the experimental trends of $H_2O$, $CO_2$ and $CH_4$ concentration effects. Besides no significant correlation occurs between the parameters also thanks to the given constraint on $CH_4$ reaction order. A statistical $F$-test on model adequacy was not attempted due to uncertainties on the variance estimate which might be biased by a slight deactivation occurred during the experimental campaign, however, the value of the mean square error is satisfactorily low. Concerning the general consistency of the parameter estimates it is worth noting that the negative reaction order $-0.32$ of $H_2O$ is markedly higher than the typical value of $-1$ reported by many authors [9–11]. This can be associated with the higher temperature range herein considered at which the inhibition effect of water, possibly due to active site blocking, is mitigated although not completely eliminated. The estimate of

Table 1
Power law rate equation (5): parameter estimates with 95% confidence limits, correlation matrix and statistical indexes (number of degrees of freedom is 49, MSE = 3.5946E + 00)

| | Parameter estimates | | |
|---|---|---|---|
| | Lower limit | Estimated value | Upper limit |
| $\beta_{11}$ | −9.94039E−01 | −6.97808E−01 | −4.01578E−01 |
| $\beta_{12}$ | 1.25766E+01 | 1.29418E+01 | 1.29418E+01 |
| *a* | 3.00021E−01 | 3.22046E−01 | 3.44071E−01 |
| *b* | 2.30263E−01 | 2.50017E−01 | 2.69771E−01 |
| *Correlation matrix* | | | |
| 1.00000E+00 | | | |
| −8.13919E−01 | 1.00000E+00 | | |
| −8.38086E−01 | 5.88183E−01 | 1.00000E+00 | |
| −8.38925E−01 | 5.73484E−01 | 4.74082E−01 | 1.00000E+00 |

the apparent activation energy ($E_{att} = 108\,\mathrm{kJ/mol}$) is lower than the value of 150 kJ/mol reported by other authors [11,22] who considered the inhibiting effect of $H_2O$. This is consistent with a mitigated effect of $H_2O$ inhibition in the high temperature range.

To attempt a more physically sound analysis of kinetic data the following expression was tested:

$$r\ (\mathrm{cm^3/g_{cat}/s\ at\ STP}) = \frac{k_c P_{CH_4}}{1 + K_{H_2O}P_{H_2O} + K_{CO_2}P_{CO_2}} \qquad (6)$$

which in principle could account for zeroth-order dependence on $O_2$ concentration, first-order dependence on $CH_4$ concentration and fractional negative reaction order on product concentrations emerged from the power law analysis. This model is consistent with a simplified mechanism proposed in the literature, assuming dissociative adsorption of $CH_4$ on an active site consisting of a coordinatively unsaturated $Pd^{2+}O^{2-}$ ion pair [22,25] as the rate determining step. The fraction of free active sites $\theta_v$ in the resulting rate expression

$$r = k_c P_{CH_4}\theta_v \qquad (7)$$

can be evaluated considering a pseudo-equilibrium condition for water, as usually done [12,13,22], and carbon dioxide adsorption. This latter must be

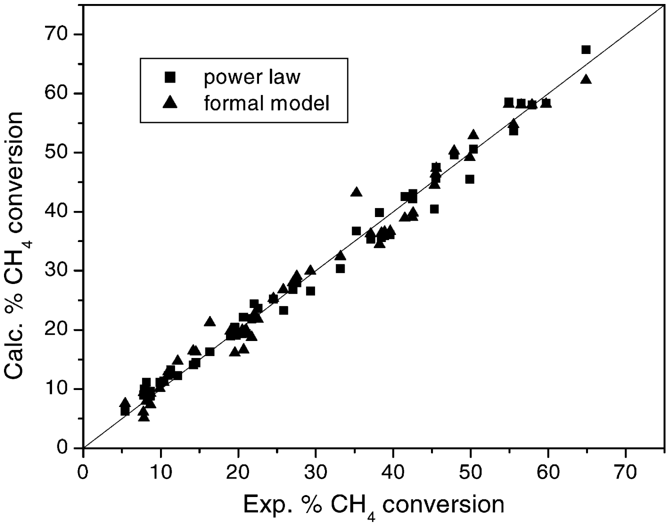

Fig. 8. Parity plot.

considered to account for the observed inhibiting effect of $CO_2$. On the other hand, the fractional site coverage due to adsorbed $CH_4$ can be reasonably neglected. Accordingly

$$\theta_v = \frac{1}{1 + K_{H_2O} P_{H_2O} + K_{CO_2} P_{CO_2}} \tag{8}$$

which substituted in (7) gives the rate expression (6).

It is worth noting that rate equation (6) can be derived either via a classical Langmuir–Hinshelwood–Hougen–Watson approach or with a Mars–van Krevelen-type mechanism assuming a slow catalyst reduction controlled by surface reaction between $CH_4$ and PdO, with competitive adsorption of $CO_2$ and $H_2O$ on the oxidised sites, followed by fast re-oxidation of surface vacancies. Evidences in favour of a Mars–van Krevelen-type mechanism were reported by Baiker and co-workers [26,27] and more recently by Pfefferle and co-workers [28]. On the basis of isotopic oxygen distribution in combustion products during pulse experiments with labelled reaction mixtures these latter authors proposed that re-oxidation uses both bulk and gas phase oxygen and also oxygen from the $ZrO_2$ support.

An expression consistent with a Mars–van Krevelen redox mechanism involving the activation of methane on a site pairs consisting of oxygen atoms and oxygen vacancies on the surface of $PdO_x$ crystallites was also proposed by Fujimoto et al. [10]. Such an expression was not herein considered since, in contrast with the collected experimental evidences, vacancies development would result in a negative reaction order with respect to $O_2$, unless surface hydroxyls originating either from surface oxidation of adsorbed $CH_4$ or from dissociative adsorption of $H_2O$ can be assumed as the most abundant surface intermediate. In this case, as shown in [10], the rate equation simplifies in a power law expression with reaction order −1 with respect to $H_2O$, which is at variance with the results of the power law analysis described above.

Table 2 provides the estimates of the six parameters in rate equation (6) (note that for temperature-dependent kinetic constant $k_c$ and thermodynamic constants $K_{H_2O}$ and $K_{CO_2}$, reparameterization formulas (3) and (4) were adopted, respectively) along with some statistical indexes provided by the regression routine. Regression results show that the model cannot be rejected neither on the basis of rigorous statistical analysis nor in view of evident chemico-physical inconsistencies of the parameter estimates since activation energy of $k_c$ ($E_{act} = 78.8\,\text{kJ/mol}$) and adsorption enthalpies of $K_{H_2O}$ and $K_{CO_2}$ ($\Delta H_{H_2O} = -29.2\,\text{kJ/mol}$, $\Delta H_{CO_2} = -54.32\,\text{kJ/mol}$) are positive and negative, respectively. However, the overall quality of the fitting seems significantly worse than that provided by the power law rate equation (5) as shown by comparison of the value of the mean square error (MSE) = 5.6255 obtained with the rate equation

Table 2
Rate equation (6): parameter estimates with 95% confidence limits, correlation matrix and statistical indexes (number of degrees of freedom is 47, MSE = 5.6255E + 00)

| | Parameter estimates | | | | |
|---|---|---|---|---|---|
| | Lower limit | Estimate | Upper limit | | |
| $\beta_{c,1}$ | 4.33581E+00 | 4.45154E+00 | 4.56727E+00 | | |
| $\beta_{c,2}$ | 8.64971E+00 | 9.17499E+00 | 9.70027E+00 | | |
| $\beta_{H_2O,1}$ | 5.62960E+00 | 5.98051E+00 | 6.33141E+00 | | |
| $\beta_{H_2O,2}$ | 2.45294E+00 | 3.99698E+00 | 5.54101E+00 | | |
| $\beta_{CO_2,1}$ | 6.34421E+00 | 6.75987E+00 | 7.17552E+00 | | |
| $\beta_{CO_2,2}$ | 5.11158E+00 | 6.96333E+00 | 8.81509E+00 | | |
| *Correlation matrix* | | | | | |
| 1.00000E+00 | | | | | |
| −9.47712E−01 | 1.00000E+00 | | | | |
| 7.76050E−01 | −7.35493E−01 | 1.00000E+00 | | | |
| 7.56835E−01 | −7.95107E−01 | 9.59819E−01 | 1.00000E+00 | | |
| 7.07803E−01 | −6.74567E−01 | 3.85232E−01 | 3.80066E−01 | 1.00000E+00 | |
| 6.85592E−01 | −7.18885E−01 | 3.75022E−01 | 4.09739E−01 | 9.62663E−01 | 1.00000E+00 |

(6) with that obtained using the power law model: MSE $= 3.5946$. Visual inspection of data fitting (see dashed lines in Figs. 5–7 and triangles in the parity plot of Fig. 8) points out the poor ability of the formal model in reproducing the saturation trend of inhibition effects exhibited by the experimental data on increasing $H_2O$ and $CO_2$ concentration, particularly at high temperature.

The relatively scarce adequacy of rate equation (6) could be associated with several reasons. First the mechanism of water inhibition/poisoning on PdO catalysts is still poorly understood. Evidences of permanent catalyst modification in the presence of feed $H_2O$ above 600 °C were obtained in this work indicating complex interaction between $H_2O$ and supported PdO. By comparing results collected under both pulsed and continuous flow conditions with and without water in the feed Ciuparu et al. [29] suggested that hydroxyl groups resulting from $CH_4$ dissociation on PdO sites could be strongly bound relative to hydroxyls resulting from water adsorption on the fully oxidised PdO surfaces. Such a complex feature could hardly be described by the single $H_2O$ adsorption equilibrium assumed in Eqs. (6) and (8). The mechanism of $CO_2$ inhibition is also scarcely understood. As stated above in this case the occurrence of an inhibition effect has been also argued. Reaction order ranging from $-2$ to 0 have been reported [9,11], the origin of such discrepancies being possibly related to the role of the support and to temperature effects. However, no detailed explanations have been reported insofar. Finally, the mechanism of $CH_4$ activation and the nature of oxygen interaction with the PdO/Pd systems are still debated [30–32].

Several others LHHW-type expressions were tried to fit the data herein presented and some of them gave a significantly better fitting than the one discussed above. However, since such expressions do not rely on reasonably assessed assumptions on reaction mechanism they represent a mere empirical fitting of the experimental data which does not provide additional information with respect to the power law expression discussed above. Accordingly, the results have not been herein reported.

More profitably detailed microkinetic model should be developed to correctly predict the catalyst behaviour providing insight on the complex features outlined above. Along these lines few attempts have been already reported in the literature [33], but further work is needed to achieve a comprehensive description of the $CH_4$/PdO–Pd combustion chemistry also in view of the lack of reliable experimental data collected under relevant high temperature conditions.

## 4. Conclusions

$CH_4$ combustion over highly active PdO-supported catalysts provide a good example of the still critical need of advanced experimental tools and deeper insight on surface reaction chemistry to obtain reliable and physically sound kinetics.

The use of an annular flow microreactor was shown to have good potential to provide unbiased kinetic data under severe conditions relevant to practical application in view of the following properties associated with its peculiar structure: (i) possibility to achieve extremely short contact times with negligible pressure drops thanks to the straightforward laminar flow pattern; (ii) control and minimisation of mass transfer effects through catalyst design and preparation; (iii) effective dissipation of reaction heat through radiation; (iv) analogy with structured catalyst adopted in industrial applications. Along these lines other similar micro-devices based on the use of appropriate catalyst structures can be conceived.

Thanks to the performances of the annular reactor a kinetic study has been performed covering an unusually high temperature range (400–550 °C). The presence of significant inhibition effects of both $H_2O$ and $CO_2$ up to 550 °C has been pointed out.

The kinetic data have been analysed according to both a power-law approach and to a formal model derived from mechanism assumptions. The comparison between the two models has shown that further insight on surface chemistry is needed in order to obtain a truly physically sound kinetic description.

## Acknowledgements

Financial support for this work has been provided by MIUR Rome—PRIN "High activity catalysts for methane lean combustion".

## References

[1] M. Boudart, in: G. Ertl, H. Knozinger, J. Weitkamp (Eds.), Handbook of Heterogeneous Catalysis, VCH, Weinheim, 1997, p. 958.

[2] M. Boudart, Catal. Lett. 65 (2000) 1.

[3] R.J. Farrauto, R.M. Heck, Catal. Today 51 (1999) 351.

[4] P. Forzatti, G. Groppi, Catal. Today 54 (1999) 49.

[5] R.A. Dalla Betta, K. Tsurumi, T. Shoji, R.L. Garten, US Patent 5 405 260, April 11, 1995.

[6] R.B. Anderson, K.C. Stein, J.J. Feenan, L.J.E. Hofer, Ind. Eng. Chem. 53 (1961) 809.

[7] C.F. Cullis, T.G. Nevell, D.L. Trimm, J. Chem. Soc., Faraday Trans. 1 (1972).

[8] Y.Y. Yao, Ind. Eng. Prod. Res. Dev. 19 (1980) 293.

[9] F.H. Ribeiro, M. Chow, R.A. Dalla Betta, J. Catal. 146 (1994) 537.

[10] K. Fujimoto, F.H. Ribeiro, M. Avalos-Borja, E. Iglesia, J. Catal. 179 (1998) 431.

[11] C. van Giezen, F.R. van den Berg, J.L. Kleinen, A.J. van Dillen, J.W. Geus, Catal. Today 47 (1999) 287.

[12] R. Kikuchi, S. Maeda, K. Sasaki, S. Wennerstrom, K. Eguchi, Appl. Catal. A 232 (2002) 23.

[13] G. Groppi, W. Ibashi, M. Valentini, P. Forzatti, Chem. Eng. Sci. 56 (2001) 831.

[14] J.G. McCarty, Catal. Today 26 (1995) 283.

[15] A. Beretta, P. Baiardi, D. Prina, P. Forzatti, Chem. Eng. Sci. 54 (1999) 765.

[16] W. Ibashi, G. Groppi, P. Forzatti, Catal. Today, submitted for publication.

[17] R.A. Dalla Betta, K. Tsurumi, T. Shoji, R.L. Garten, US Patent 5 259 754, November 9, 1993.

[18] D.E. Mears, Ind. Eng. Chem. Process. Des. Develop. 10 (1971) 541.

[19] R. Burch, F.J. Urbano, P.K. Loader, Appl. Catal. A 123 (1995) 173.

[20] K. Nomura, K. Noro, Y. Nakamura, H. Yoshida, A. Tsatsuma, T. Hattori, Catal. Lett. 58 (1999) 127.

[21] R.A. Dalla Betta, J.C. Schlatter, D.K. Yee, D.G. Loffler, T. Shoji, Catal. Today 26 (1995) 329.

[22] D. Ciuparu, L. Pfefferle, Appl. Catal. A 209 (2001) 415.

[23] G. Donati, G. Buzzi Ferraris, Chem. Eng. Sci. 29 (1974) 1504.

[24] P.L. Villa, P. Forzatti, G. Buzzi Ferraris, G. Garone, I. Pasquon, Ind. Eng. Chem. Prod. Res. Develop. 24 (1985) 12.

[25] E. Broclawik, R. Yamauchi, A. Endou, M. Kubo, A. Miyamoto, J. Chem. Phys. 104 (1996) 4098.

[26] C. Muller, M. Maciejewski, R. Koeppel, R. Tschan, A. Baiker, J. Phys. Chem. 100 (1996) 20006.

[27] C. Muller, M. Maciejewski, R. Koeppel, A. Baiker, Catal. Today 47 (1999) 245.

[28] D. Ciuparu, E. Altman, L. Pfefferle, J. Catal. 203 (2001) 64.

[29] D. Ciuparu, N. Katsikis, L. Pfefferle, Appl. Catal. A 216 (2001) 209.

[30] Y.H. Chin, D. Resasco, Catalysis 14 (1999) 1.

[31] G. Centi, J. Mol. Catal. A 173 (2001) 287.

[32] T.V. Choudhari, S. Banerjee, V.R. Choudary, Appl. Catal. A 234 (2002) 1.

[33] H. Zhu, G.S. Jackson, ASME Paper 2001-GT-520.